

# Zinc Overload Enhances APP Cleavage and A $\beta$ Deposition in the Alzheimer Mouse Brain

Chun-Yan Wang<sup>1</sup>, Tao Wang<sup>1</sup>, Wei Zheng<sup>1</sup>, Bao-Lu Zhao<sup>2</sup>, Gorm Danscher<sup>3</sup>, Yu-Hua Chen<sup>1\*</sup>, Zhan-You Wang<sup>1\*</sup>

**1** Key Laboratory of Cell Biology of Ministry of Public Health, and Key Laboratory of Medical Cell Biology of Ministry of Education, China Medical University, Shenyang, China, **2** State Key Laboratory of Brain and Cognitive Sciences, Institute of Biophysics, Academia Sinica, Beijing, China, **3** Department of Anatomy and Neurobiology, University of Aarhus, Aarhus, Denmark

## Abstract

**Background:** Abnormal zinc homeostasis is involved in  $\beta$ -amyloid (A $\beta$ ) plaque formation and, therefore, the zinc load is a contributing factor in Alzheimer's disease (AD). However, the involvement of zinc in amyloid precursor protein (APP) processing and A $\beta$  deposition has not been well established in AD animal models *in vivo*.

**Methodology/Principal Findings:** In the present study, APP and presenilin 1 (PS1) double transgenic mice were treated with a high dose of zinc (20 mg/ml ZnSO<sub>4</sub> in drinking water). This zinc treatment increased APP expression, enhanced amyloidogenic APP cleavage and A $\beta$  deposition, and impaired spatial learning and memory in the transgenic mice. We further examined the effects of zinc overload on APP processing in SHSY-5Y cells overexpressing human APP<sub>sw</sub>. The zinc enhancement of APP expression and cleavage was further confirmed *in vitro*.

**Conclusions/Significance:** The present data indicate that excess zinc exposure could be a risk factor for AD pathological processes, and alteration of zinc homeostasis is a potential strategy for the prevention and treatment of AD.

**Citation:** Wang C-Y, Wang T, Zheng W, Zhao B-L, Danscher G, et al. (2010) Zinc Overload Enhances APP Cleavage and A $\beta$  Deposition in the Alzheimer Mouse Brain. PLoS ONE 5(12): e15349. doi:10.1371/journal.pone.0015349

**Editor:** Ashley I. Bush, Mental Health Research Institute of Victoria, Australia

**Received:** August 12, 2010; **Accepted:** November 11, 2010; **Published:** December 17, 2010

**Copyright:** © 2010 Wang et al. This is an open-access article distributed under the terms of the Creative Commons Attribution License, which permits unrestricted use, distribution, and reproduction in any medium, provided the original author and source are credited.

**Funding:** The study was supported by the Natural Science Foundation of China (30770680), the Program for New Century Excellent Talents in University (NCET-04-0288), the Research Project for Universities of the Department of Education of Liaoning Province (20060948), and the National Basic Research Program of China (973 Program 2009CB930300). The funders had no role in study design, data collection and analysis, decision to publish, or preparation of the manuscript.

**Competing Interests:** The authors have declared that no competing interests exist.

\* E-mail: zhanyouw@hotmail.com (Z-YW); yhchen@mail.cmu.edu.cn (Y-HC)

## Introduction

The presence of extracellular  $\beta$ -amyloid (A $\beta$ ) plaques in the brain is one of the pathological hallmarks of Alzheimer's disease (AD). Mounting evidence has demonstrated that aberrant zinc homeostasis is involved in the pathogenesis of AD [1,2,3,4]. In the post-mortem AD brain, a marked accumulation of zinc is found in the A $\beta$  plaques [5,6,7,8,9,10]. Since A $\beta$  peptide has zinc-binding sites, and zinc is the only physiologically available metal able to precipitate A $\beta$ , the abnormal enrichment of zinc in the AD brain indicates that zinc binding to A $\beta$  plays a role in the formation of amyloid plaques [11]. Furthermore, zinc chelating agents, such as clioquinol (CQ) and DP-109, that modulate brain zinc levels can inhibit the formation of amyloid plaques [12,13,14]. In preliminary studies, CQ has shown some effects on cognition in AD patients [15,16,17]. Thus, abnormal zinc homeostasis is believed to be a contributing factor leading to A $\beta$  aggregation, and alteration of zinc homeostasis is a potential therapeutic strategy for AD.

The disruption of zinc homeostasis in the AD brain is associated with the aberrant distribution and altered expression of zinc-regulating metalloproteins, such as metallothionein, zinc transporters (ZnT) and divalent metal transporter 1 (DMT1). We have reported that high levels of ZnT1, 3-7 and DMT1 proteins are

located in the degenerating neurites in or around the A $\beta$ -positive plaques associated with human AD and the APP/presenilin 1 (PS1) transgenic mouse brain [18,19,20,21]. Significant alterations in the expression levels of ZnT1, 4, and 6 have been detected in AD postmortem brain specimens [22,23]. Genetic abolition of ZnT3 results in disappearance of zinc ions in the synaptic vesicles [24], and leads to an age-dependent deficit in learning and memory in ZnT3 knockout mice [25]. Most interestingly, a markedly reduced plaque load and less insoluble A $\beta$  have been observed in ZnT3 knockout plus APP overexpressed mouse brain [26], suggesting a role of synaptic zinc in A $\beta$  generation and aggregation. Furthermore, *in vitro* studies have shown that both APP and its proteolytic product A $\beta$  contain zinc binding domains. However, the involvement of zinc in APP processing and A $\beta$  deposition has not been well established in AD transgenic models *in vivo*.

In the present study, we extended our experiments to examine whether chronic intake of water containing a high level of zinc accelerates A $\beta$  deposition and APP cleavage in APP/PS1 mouse brain. We found that a high level of dietary zinc could cause cognition dysfunction and enhance the aggregation of A $\beta$ . Furthermore, we found that a high level of zinc also enhanced A $\beta$  generation through altering the expression levels of APP and APP cleavage enzymes *in vivo* and *in vitro*. Our data support the

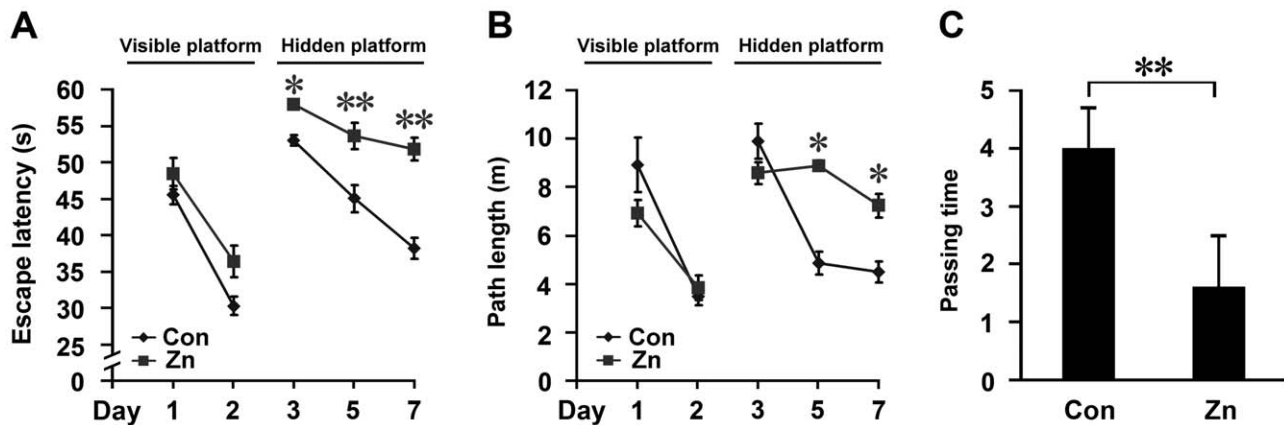


**Figure 1. Morris water maze assessment of APP/PS1 transgenic mice.** APP/PS1 mice at the age of 3 months were given either a standard diet and deionized water (Con), or a standard diet and deionized water containing 20 mg/ml ZnSO<sub>4</sub> (Zn). Morris water maze tests were performed to evaluate whether high dietary zinc treatment affects learning and memory in APP/PS1 mice at the age of 9 months. (A, B) In the visible platform training from day 1 to 2, mice in different groups exhibited a similar escape latency and path length to find the visible platform. At day 3, 5, and 7 of the hidden platform tests, Zn-treated mice showed the longest latency and escape length. (C) In the probe trial on the last day, the Zn-treated mice exhibited the lowest passing times into the northwest quadrant, where the hidden platform was previously located. \*  $p < 0.05$ , \*\*  $p < 0.01$  versus control group (repeated measures ANOVA). doi:10.1371/journal.pone.0015349.g001

possibility that dietary zinc overload has the potential to be a contributing factor to the pathophysiology of AD.

## Results

### Chronic high intake of dietary zinc induces spatial learning-memory deficits in APP/PS1 mice

APP/PS1 transgenic mice at the age of 3 months were given a standard diet and deionized water containing ZnSO<sub>4</sub> (20 mg/ml). Morris water maze tests were performed to evaluate whether high dietary zinc treatment affects learning and memory in APP/PS1 mice at the age of 9 months. These included 2 days of visible platform training, 5 days of hidden platform tests, and a probe trial 1 day after the last hidden platform test (Figure 1). The visible platform tests showed that the zinc group and control mice had a similar escape latency and path length ( $p > 0.05$ ; Figure 1A, B), suggesting that zinc treatment did not significantly affect motility or vision in the transgenic mice. In the place navigation (hidden platform) tests, the zinc group mice showed a longer escape latency and a longer path length before swimming onto the hidden platform compared with the control mice fed a normal diet ( $p < 0.01$ ; Figure 1A, B). Furthermore, the probe trial showed that the number of times the mice traveled into the center of the northwest quadrant, where the hidden platform was previously placed, was significantly less for zinc group mice compared with controls ( $p < 0.01$ ; Figure 1C). Taken together, these data suggest that high-dose oral zinc leads to spatial learning-memory impairments in APP/PS1 mice.

### Enhancement of zinc content in serum and brain of APP/PS1 mice fed a zinc diet

The serum zinc levels were measured in the transgenic mice at the age of 9 months. There was a significant increase in zinc level in the zinc group ( $11.21 \pm 2.42$   $\mu\text{g/ml}$ ), compared with the control ( $0.43 \pm 0.12$   $\mu\text{g/ml}$ ) ( $p < 0.01$ ; Figure 2A). We also measured the zinc level in the brain of the transgenic mice to determine the effects of a high zinc diet. The brain zinc level was  $173.17 \pm 24.72$  ng/mg in the zinc group, and  $23.59 \pm 2.31$  ng/mg in the control group. Statistical analysis showed that treatment

with a high dose of zinc significantly increased the level of zinc in the brain ( $p < 0.01$ ; Figure 2B).

### Increase in the number of zinc-containing plaques in the brain of APP/PS1 mice fed a high zinc diet

The autometallography (AMG) procedure allows demonstration of a striking condensation of ionic zinc within plaques in the human postmortem AD brain and the APP/PS1 transgenic mouse brain [10,19]. Brain sections of APP/PS1 mice given a high dose of zinc in their drinking water and normal diet were subjected to AMG analysis. In general, zinc-positive plaques were distributed throughout the cortex and hippocampus in all examined animals (Figure 3A), as previously described [27]. Both the number and size of the zinc-positive plaques in the zinc-treated group were markedly increased in the cortex and hippocampus (Figure 3A). Statistical analyses showed that high zinc treatment significantly increased the number of zinc-positive plaques by  $146.24 \pm 12.30\%$  in the cortex and  $225.00 \pm 22.97\%$  in the hippocampus respectively, compared with the control group ( $p < 0.01$ ; Figure 3B). The size of zinc-containing plaques in the brain of APP/PS1 mice fed a high zinc diet was increased by  $186.83 \pm 15.74\%$

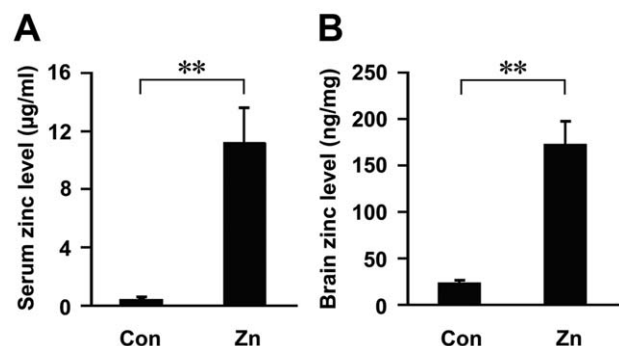


**Figure 2. Changes in zinc level in APP/PS1 mice fed a zinc diet.** (A) At the age of 9 months, the Zn group mice showed an increased level of serum zinc. (B) Brain zinc levels were also significantly increased in the Zn group mice. \*\*  $p < 0.01$  versus control group (Student's *t* test). doi:10.1371/journal.pone.0015349.g002

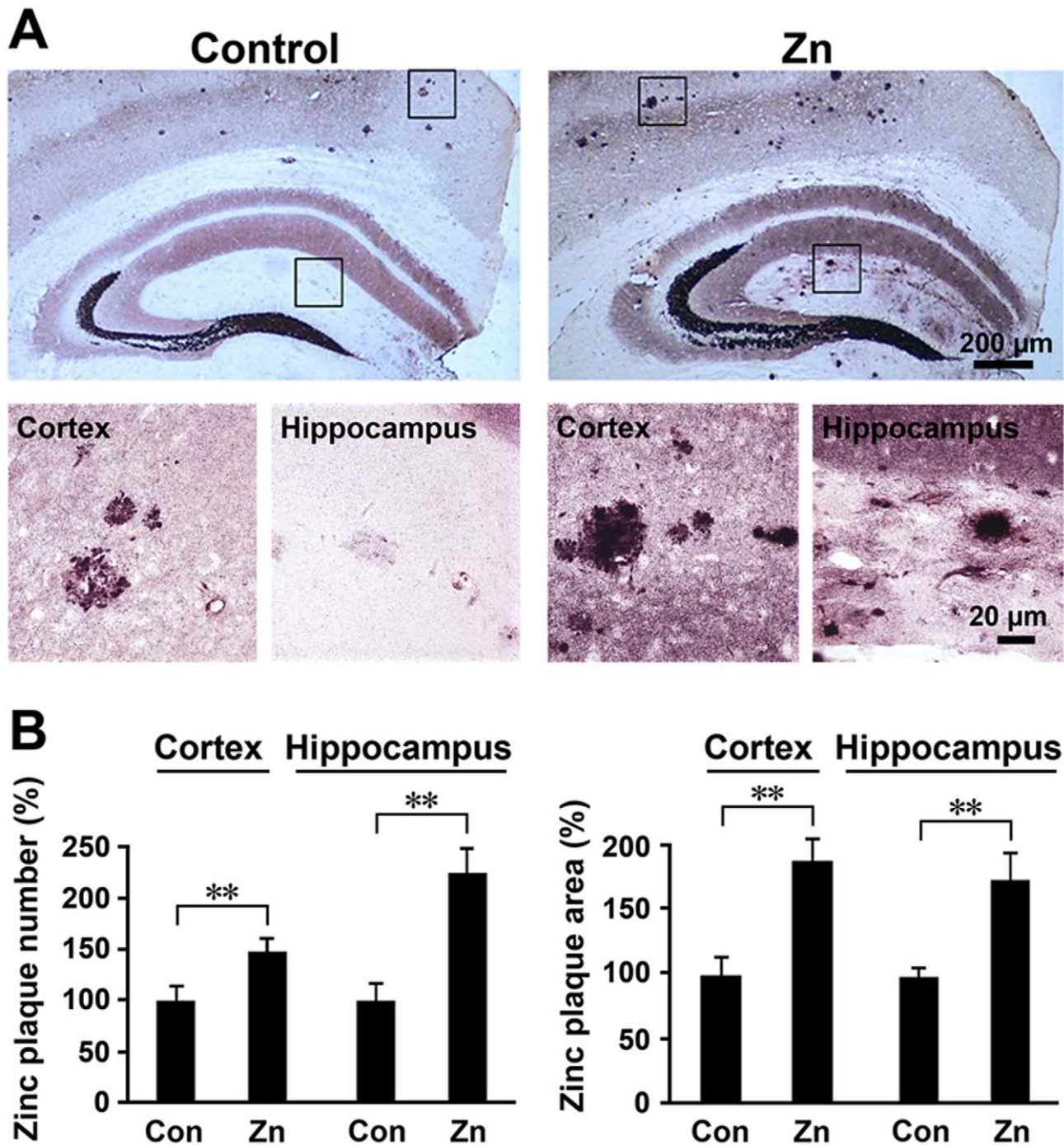


**Figure 3. Zinc accumulation in neuritic plaques in APP/PS1 mice.** (A) Zinc ions stained by AMG showing the distribution patterns of zinc ions in the cortex and hippocampus, especially mossy fibers. Importantly, the number and size of the zinc-containing plaques were increased in Zn-treated mice. (B) Statistical analysis showing that the number and size of zinc-containing neuritic plaques were significantly increased in Zn-treated mice compared with controls. \*\*  $p < 0.01$  versus control group (Student's  $t$  test). doi:10.1371/journal.pone.0015349.g003

in the cortex and  $179.60 \pm 21.74\%$  in the hippocampus, compared with the control group ( $p < 0.01$ ; Figure 3B).

#### High dietary zinc increases A $\beta$ burden in the APP/PS1 mouse brain

To determine whether chronic high intake of dietary zinc potentiates A $\beta$  deposition, brain sections of APP/PS1 mice were

subjected to A $\beta$  immunohistochemical analysis. As shown in Figure 4, both the number and size of the A $\beta$ -immunoreactive senile plaques were markedly increased in the cortex and hippocampus in the brain of zinc-treated mice (Figure 4A). Statistical analyses showed that a high intake of dietary zinc significantly increased the number of A $\beta$  plaques by  $154.55 \pm 8.25\%$  in the cortex and  $188.31 \pm 11.90\%$  in the hippocampus, compared with the control group fed a normal diet

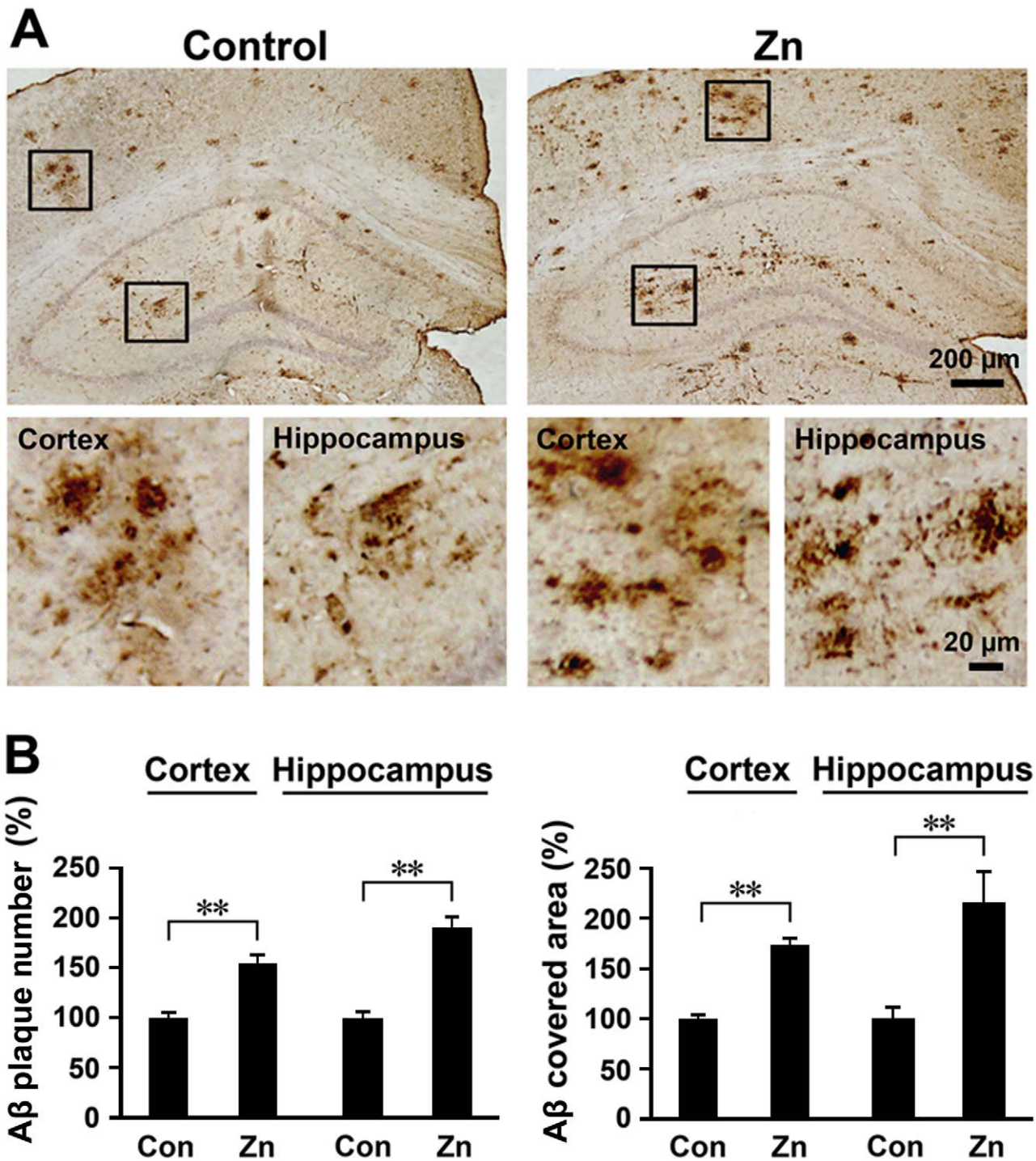


**Figure 4. Zinc treatment enhances neuritic plaque formation in APP/PS1 mice.** (A) Aβ immunohistochemical images showing the Aβ-positive plaques in the transgenic mouse brain. There were more neuritic plaques in Zn-treated mice compared with controls. (B) Quantification of neuritic plaques showed that both the number and size of neuritic plaques were increased in Zn-treated mice compared with controls. \*\*  $p < 0.01$  versus control group (Student's  $t$  test). doi:10.1371/journal.pone.0015349.g004

( $p < 0.01$ ; Figure 4B). We also evaluated the changes in Aβ burden by measuring the areas of Aβ-positive neuritic plaques in the mouse brain. In the zinc group, the area of Aβ plaques was significantly increased by  $173.36 \pm 11.44\%$  in the cortex and  $213.15 \pm 34.29\%$  in the hippocampus, compared with the control group ( $p < 0.01$ ; Figure 4B).

Increase in expression level of APP protein and Aβ generation in the APP/PS1 mouse brain after a high zinc diet

To further test whether a high dose of dietary zinc affects APP expression, the levels of APP mRNA and APP695 protein were measured by RT-PCR and Western blotting, respectively. As can

be seen in Figure 5A, the expression levels of APP mRNA were not significantly changed between groups after examining brain samples of APP/PS1 mice treated with zinc or fed a normal diet. Western blot analysis revealed that zinc treatment significantly increased the level of APP695 protein by  $132.79 \pm 16.82\%$ , compared with controls fed a normal diet (Figure 5B).

To determine whether a high zinc intake had altered brain A $\beta$  levels in APP/PS1 mice, a Sandwich ELISA for the detection of A $\beta$  was employed (Figure 5C, D). Statistical analysis showed that a high zinc diet significantly increased the level of A $\beta$ 1-40 ( $p < 0.05$ ) and A $\beta$ 1-42 ( $p < 0.01$ ) in the brain, compared with controls. The levels of A $\beta$ 1-40 and A $\beta$ 1-42 were increased by  $122.19 \pm 20.60\%$  (Figure 5C) and by  $148.96 \pm 15.67\%$  (Figure 5D) in the brain homogenates of APP/PS1 mice with a high level of zinc in their drinking water, compared with controls fed a normal diet.

#### High level of zinc in drinking water accelerates APP processing in the APP/PS1 mouse brain

To further examine whether a high intake of dietary zinc altered APP processing, the relative key enzymes (including ADAM10,

BACE1 and PS1) and cleavage fragments of APP (including sAPP $\alpha$ , sAPP $\beta$ , C83 and C99) in the brain samples of APP/PS1 mice were subjected to Western blot analyses. As shown in Figure 6A, zinc treatment significantly decreased the expression level of ADAM10 by  $45.80 \pm 7.01\%$  compared with the control group ( $p < 0.01$ ; Figure 6A). In contrast, the level of BACE1 was significantly increased in zinc-treated mouse brain by  $147.49 \pm 21.91\%$  ( $p < 0.01$ ; Figure 6A). Furthermore, the level of PS1 in zinc-treated mouse brain was significantly increased by  $130.44 \pm 36.80\%$ , compared with the control group ( $p < 0.01$ ; Figure 6A).

We then examined the levels of  $\alpha$ -secretase-generated sAPP $\alpha$ /C83 and  $\beta$ -secretase-generated sAPP $\beta$ /C99 fragments in the transgenic mouse brain. Zinc treatment significantly reduced the level of sAPP $\alpha$  by  $53.55 \pm 3.32\%$  ( $p < 0.01$ ; Figure 6B), and increased the level of sAPP $\beta$  by  $255.62 \pm 27.24\%$ , compared with the control group ( $p < 0.01$ ; Figure 6B). The level of C83 fragments was reduced by  $70.48 \pm 4.27\%$  and the level of C99 was increased by  $144.65 \pm 15.79\%$  in brain of zinc-treated mice relative to the controls ( $p < 0.01$ ; Figure 6B).

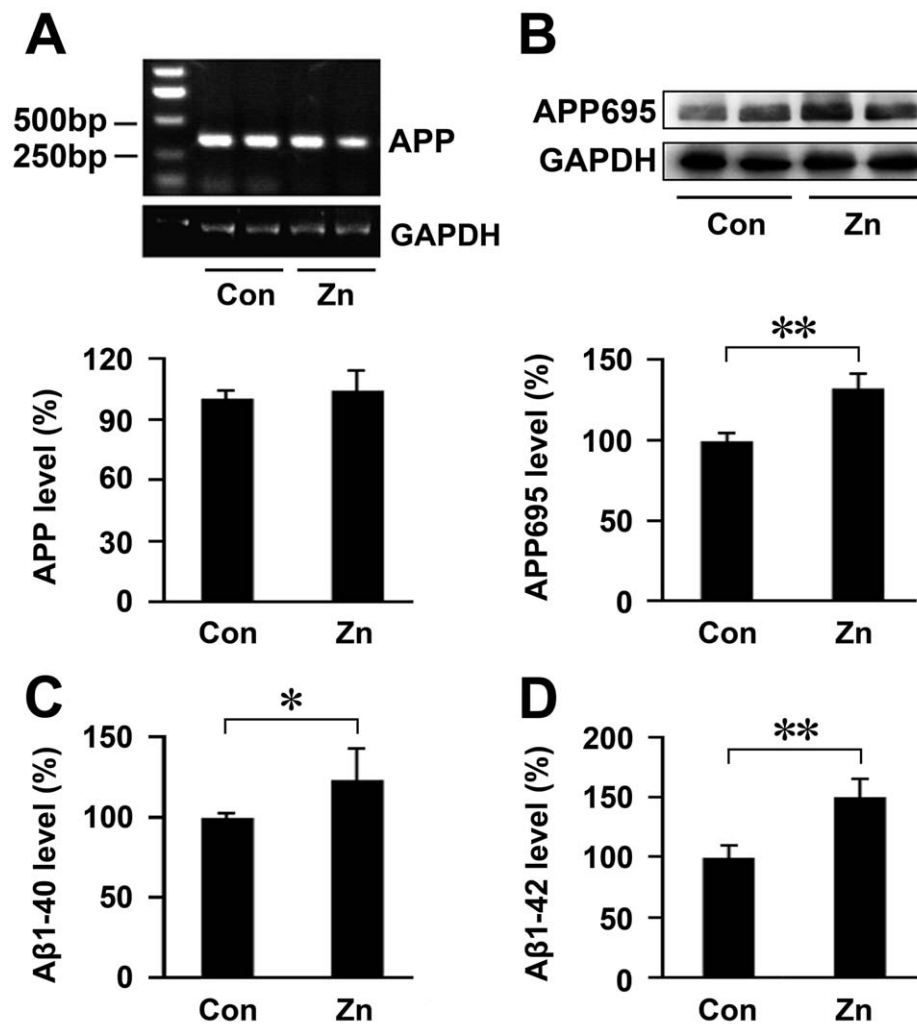


**Figure 5. Expression level of APP and A $\beta$  in APP/PS1 mice.** (A) RT-PCR showed that no difference in APP mRNA levels between groups was detected in the transgenic mouse brain. GAPDH was used as an internal control. (B) Western blot analysis showed that high zinc treatment significantly increased the level of APP695 protein. GAPDH was used as an internal control. (C, D) ELISA assay showed that the levels of A $\beta$ 1-40 and A $\beta$ 1-42 were significantly increased in Zn-treated mice compared with controls. \*  $p < 0.05$ , \*\*  $p < 0.01$  versus control group (Student's *t* test). doi:10.1371/journal.pone.0015349.g005

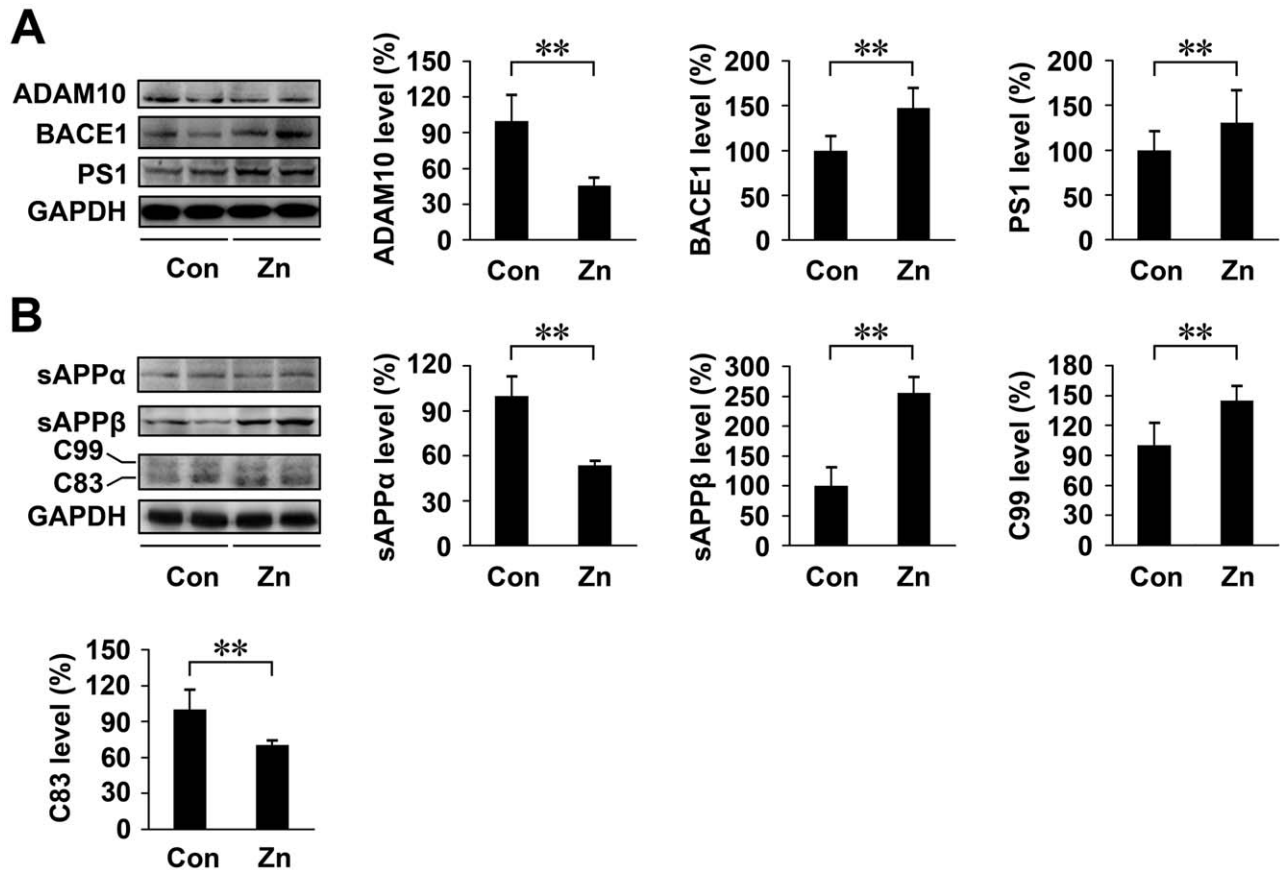


**Figure 6. Expression level of APP cleavage enzymes and products in APP/PS1 mice.** (A) The expression levels of ADAM10, BACE1 and PS1 in transgenic mouse brain were determined by Western blot analyses. GAPDH was used as an internal control. The level of ADAM10 was markedly reduced, whereas the level of BACE1 was significantly increased in Zn-treated mice, compared with controls. (B) Zinc treatment significantly reduced the level of sAPP $\alpha$  and C83, and increased the level of sAPP $\beta$  and C99 compared with the control group. \*\*  $p < 0.01$  versus control group (Student's t test).

doi:10.1371/journal.pone.0015349.g006

Taken together, these results indicate that the  $\alpha$ -secretase cleavage activity is markedly reduced while  $\beta$ - and  $\gamma$ -secretase are increased in the brain of zinc-treated transgenic mice.

#### High zinc exposure enhances amyloidosis in APPsw transfected cells

To further verify that high zinc exposure might be involved in APP processing and A $\beta$  secretion, a human neuroblastoma SHSY-5Y cell line stably transfected with APPsw was used as an *in vitro* model [28,29]. A zinc concentration of 1  $\mu$ M (low zinc) and 70  $\mu$ M (high zinc), and a concentration of TPEN (zinc chelator) of 1  $\mu$ M were selected based on the evaluation of cell viability by MTT assay (Figure 7A, B). The zinc-specific fluorescent probe, Zinquin, was used to examine the levels of zinc in cells after zinc or chelator treatments. The results showed that Zinquin fluorescence was distributed in a punctate pattern in APPsw cells (Figure 7C). Zinc treatments increased the Zinquin fluorescence, while TPEN reduced it (Figure 7C). The fluorescence density assays showed that 70  $\mu$ M zinc treatment significantly enhanced the Zinquin fluorescence by  $300.31 \pm 56.19\%$  ( $p < 0.01$ ; Figure 7D), whereas TPEN treatment reduced the fluorescence density by  $30.94 \pm 14.65\%$  compared with the control cultures ( $p < 0.01$ ; Figure 7D).

Consistent with our *in vivo* data from APP/PS1 transgenic mice, high zinc (70  $\mu$ M) exposure significantly increased the APP

cleavage enzyme levels of BACE1 by  $135.50 \pm 17.05\%$  and PS1 by  $132.79 \pm 13.11\%$  ( $p < 0.01$ ), and reduced the levels of ADAM 10 by  $80.11 \pm 5.04\%$  ( $p < 0.05$ ), respectively, in APPsw cells (Figure 8A). Subsequently, the levels of  $\beta$ -secretase-generated fragments sAPP $\beta$  and C99 were markedly increased by  $131.46 \pm 8.57\%$  and  $126.95 \pm 22.46\%$  ( $p < 0.01$ ), while the levels of  $\alpha$ -secretase-generated sAPP $\alpha$  and C83 were decreased by  $79.89 \pm 4.63\%$  ( $p < 0.01$ ) and  $76.94 \pm 5.61\%$  ( $p < 0.05$ ), respectively, following 70  $\mu$ M zinc treatment (Figure 8B). Also, chelation of zinc with 1  $\mu$ M TPEN reversed the changes in the expression levels of the cleavage enzymes and fragments of APP (Figure 8B). Furthermore, ELISA detection showed that the levels of secreted A $\beta$ 1-42 in culture medium were increased by  $166.27 \pm 23.04\%$  in the 70  $\mu$ M zinc treatment group ( $p < 0.01$ ; Figure 8C), and reduced by  $37.18 \pm 10.36\%$  with 1  $\mu$ M TPEN ( $p < 0.01$ ; Figure 8C), compared with the control group. These data clearly indicated that high zinc exposure enhanced the amyloidogenic APP cleavage pathway and A $\beta$  generation in APPsw overexpressing cells.

In contrast to high zinc exposure, low zinc (1  $\mu$ M) treatment guided APP processing to the non-amyloidogenic pathway in our APPsw overexpressing cells. Following 1  $\mu$ M zinc treatment, the levels of AMAM10, sAPP $\alpha$  and C83 were increased by  $142.21 \pm 12.04\%$  ( $p < 0.05$ ; Figure 8A),  $116.71 \pm 19.07\%$  ( $p < 0.05$ ; Figure 8B) and  $117.81 \pm 12.47\%$  ( $p < 0.05$ ; Figure 8B), whereas the

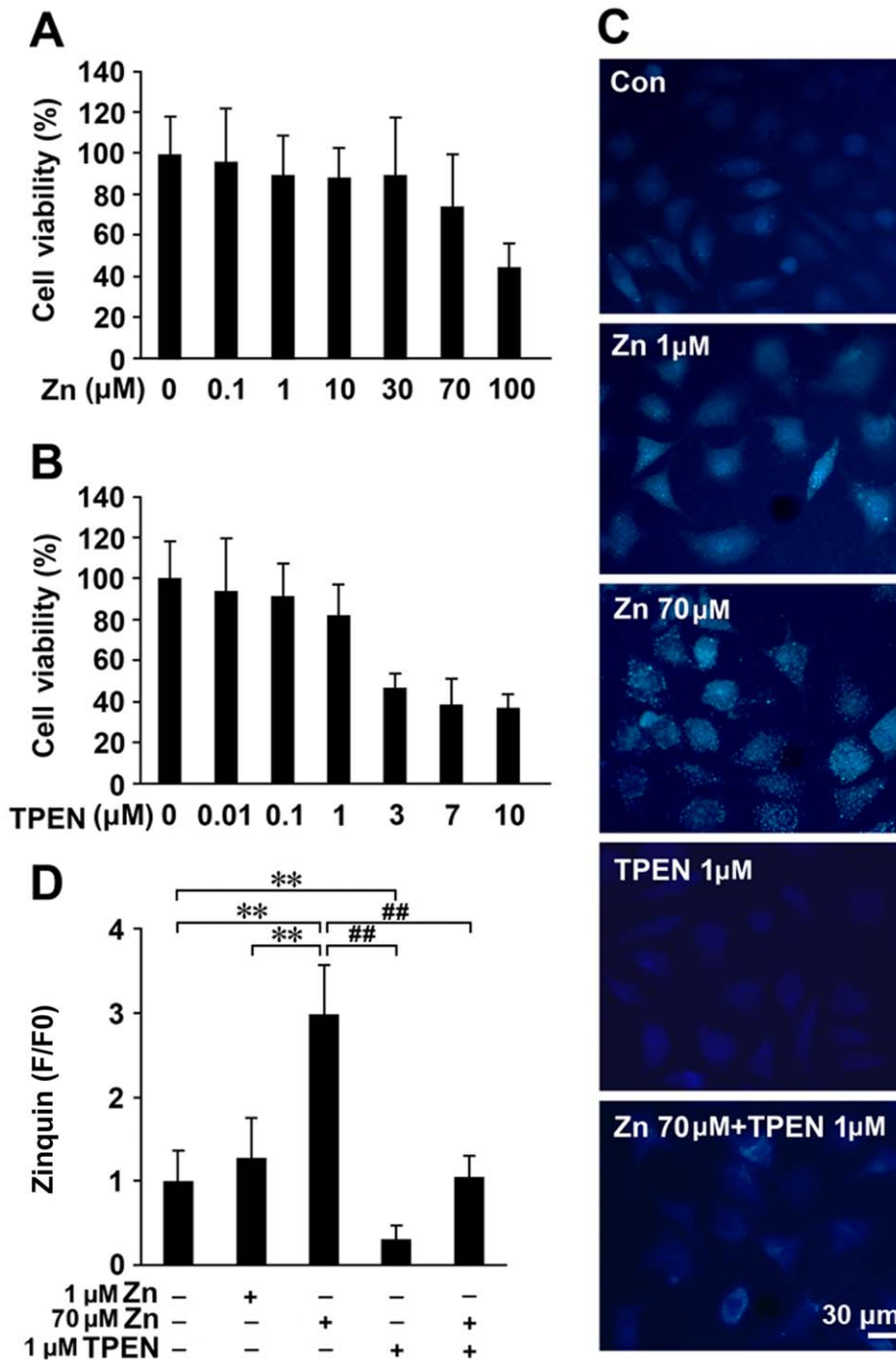


**Figure 7. Cell viability and zinc accumulation in APPsw cells treated with zinc and TPEN.** (A, B) MTT analyses were performed on the SHSY-5Y cells stably transfected with human APPsw, to select appropriate concentrations of zinc and TPEN for the *in vitro* studies. The cells were treated with indicated concentrations of zinc and TPEN for 8 h. Based on the cell viability, we chose a concentration of 1 μM ZnSO<sub>4</sub> as “low zinc” and 70 μM as “high zinc” treatment, and 1 μM TPEN for zinc chelation treatment, respectively. (C, D) Zinquin fluorescence staining showing that zinc treatments enhanced the Zn-fluorescence accumulation, while TPEN reduced the density of fluorescence in APPsw cells. Fluorescence values were obtained during the period of basal conditions and the status at the end of each indicated administration. The y-axis data describe F/F<sub>0</sub> fluorescence values. \*\* *p*<0.01 versus control group; ## *p*<0.01 versus 70 μM Zn treatment group (one-way ANOVA *Post hoc* Fisher’s PLSD). doi:10.1371/journal.pone.0015349.g007

levels of BACE1, sAPPβ and C99 were reduced by 89.61±13.34% (*p*<0.05; Figure 8A), 81.03±4.80% (*p*<0.05; Figure 8B) and 94.06±9.89% (*p*<0.05; Figure 8B), respectively, compared with the controls. The level of secreted Aβ<sub>1-42</sub> in culture medium was decreased by 64.43±11.77%, following 1 μM zinc treatment

(*p*<0.05; Figure 8C). These data are consistent with previous reports showing that exposure to low concentrations of zinc (≤50 μM) significantly enhances the levels of secreted APP and results in reduced release of Aβ in a medium of cultured CHO-K1 cells [30,31].

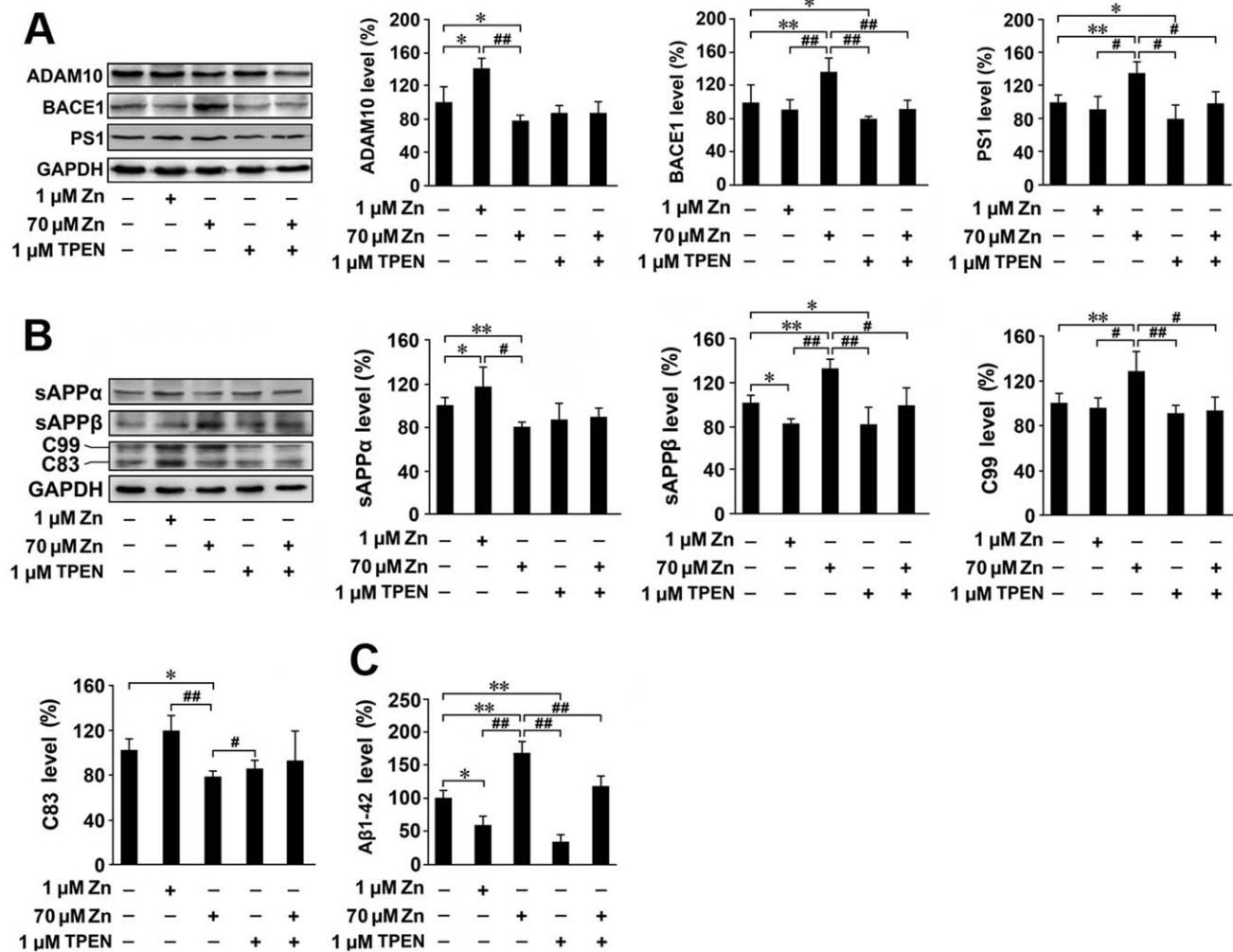


**Figure 8. Expression level of APP cleavage enzymes and products in APPsw cells.** SHSY-5Y cells stably overexpressing APPsw were exposed to 1 μM zinc, 70 μM zinc, 1 μM TPEN, and 70 μM zinc plus 1 μM TPEN, respectively, for 8 h. **(A)** Western blot was performed to determine the expression levels of APP cleavage enzymes, including ADAM10, BACE1 and PS1. GAPDH was used as an internal control. Low (1 μM) and high zinc (70 μM) treatment showed different effects on the expression of ADAM10. ADAM10 was markedly increased after low zinc treatment, but significantly reduced after high zinc treatment. There were no significant changes in ADMA10 levels in the TPEN or Zn + TPEN group, compared with controls. High zinc (70 μM) treatment significantly increased the levels of BACE1 as well as PS1. TPEN treatment reduced the BACE1 and PS1 levels. In Zn + TPEN group, the levels of BACE1 and PS1 were significantly reduced compared with the high zinc (70 μM) treatment group. **(B)** The expression levels of APP cleavage products, including sAPPα, sAPPβ, C83 and C99, were determined by Western blot analysis. GAPDH was used as an internal control. Low zinc (1 μM) exposure significantly enhanced the expression level of sAPPα, however, high zinc (70 μM) treatment markedly reduced the sAPPα expression level. There were no significant changes in sAPPα levels in the TPEN or Zn + TPEN treatment group compared with controls. The expression level of sAPPβ was significantly decreased after low zinc (1 μM) treatment, but was significantly increased after high zinc (70 μM) treatment. **(C)** ELISA results showed the Aβ1-42 level in the medium of APPsw cells following the indicated treatments. High zinc (70 μM) treatment significantly increased the levels of Aβ1-42, whereas low zinc (1 μM) and TPEN treatment reduced the levels of Aβ1-42. \*  $p < 0.05$ , \*\*  $p < 0.01$  versus control group; #  $p < 0.05$ , ##  $p < 0.01$  versus 70 μM Zn treatment group (one-way ANOVA *Post hoc* Fisher's PLSD). doi:10.1371/journal.pone.0015349.g008

## Discussion

Both APP and its proteolytic byproduct Aβ, which play central roles in senile plaque formation in the pathogenesis of AD, are zinc-containing metalloproteins that contain zinc-binding domains [32]. Therefore, it is rational to speculate that zinc overload may be involved in APP expression, Aβ generation and aggregation. In the present study, involving treatment with a high level of zinc in the drinking water of APP/PS1 mice, we found that mice fed a high zinc diet exhibited spatial learning impairments as shown by Morris water maze tests. Apart for body weight loss, fur color changes (data not shown), raised serum and brain zinc levels, and a

high zinc content in the drinking water resulted in no other overt signs of toxicity such as general behavioral and neurological changes during the entire observation period which our model mice were given a high zinc diet. This is in agreement with previous reports showing that there was no serious toxicity in C57BL/6 mice after chronic zinc treatment at the same dose [33,34]. Thus, we further evaluated the effects of a chronic high dietary zinc intake on accumulation of Aβ deposits, as well as APP expression and cleavage in the APP/PS1 transgenic mouse brain.

We and others have reported that zinc is highly concentrated in amyloid plaques in human postmortem brain samples [5,6,7,8,10,18,35] and in AD transgenic mouse brains [9,36]. Here, we

found that a high intake of dietary zinc resulted in an increase in zinc-containing plaques in APP/PS1 transgenic mice. Coincident with the AMG results, A $\beta$  immunohistochemical analyses demonstrated that there was an increased A $\beta$  burden in transgenic mice fed a high zinc diet. Since the small peptide A $\beta$  possesses selective high- and low-affinity zinc binding sites [32,37], and zinc at a concentration of 300 nM can rapidly destabilize A $\beta$  and result in fibril formation [11,37], it is likely that an overload of brain zinc increases A $\beta$  binding and, hence, enhances A $\beta$  aggregation and plaque formation in the brain after chronic administration of a high zinc diet.

Zinc is toxic and, besides its physiological roles, it is involved in neuronal and glial death through activation of multiple intracellular pathways leading to necrotic, apoptotic and autophagic neuronal death [38,39,40,41]. The elevated level of zinc in the AD brain is caused, at least partly, by the abnormal distribution and expression of zinc-regulating proteins such as ZnTs and DMT1 [18,19,21]. At an early stage of AD, the elevated brain zinc results in the formation of zinc-A $\beta$  complex, which is of some benefit in protecting against zinc toxicity [42,43,44]. On the other hand, recent studies have shown that soluble A $\beta$  is a major factor in neuronal and synaptic pathology, since it is more toxic than insoluble A $\beta$  [45,46,47]. It is likely that the initial zinc-A $\beta$  complex and subsequent A $\beta$  aggregation inhibits A $\beta$  mediated neurotoxicity. However, it is worth noting that the initial zinc-A $\beta$  complex may serve as a seed for the process of A $\beta$  aggregation and plaque formation in the brain [5,11,48,49]. Although it is still debatable whether A $\beta$  aggregation mediated by interaction with zinc plays a role in reducing the toxicity of soluble A $\beta$  or whether the zinc-containing plaques themselves are toxic to neuronal cells [44,50,51,52], the interaction between A $\beta$  and zinc seems to be a critical factor for activating AD pathological processes. Nevertheless, our present data suggest that a high zinc intake leads to more zinc-A $\beta$  complex formation, accelerates A $\beta$  deposition and enhances the amyloid burden. Further studies are needed to elucidate the paradoxical role of zinc in plaque pathology [31].

APP protein contains a novel zinc binding motif which is located between the cysteine-rich and negatively charged ectodomains [32]. Besides its structural role, zinc may be involved in the function and metabolism of APP protein, and produce an even greater deposition of A $\beta$ . However, apart for several *in vitro* studies that tested the effects of zinc on APP processing [30,53], there are no detailed reports whether zinc binding to APP alters APP processing and A $\beta$  production in AD transgenic animal models. In the present study, we found that a high intake of dietary zinc significantly increases the expression levels of APP protein in APP/PS1 transgenic mouse brain. We also found that high-dose zinc treatment results in reduced expression levels of ADAM10, but enhances the levels of BACE1 and PS1, resulting in increased secretion of sAPP $\beta$  over sAPP $\alpha$  in the transgenic mouse brain. Further, consistent with our *in vivo* data, high zinc (70  $\mu$ M) exposure suppresses  $\alpha$ -secretase cleavage, but enhances  $\beta$ - and  $\gamma$ -secretase cleavage of APP and A $\beta$  generation in APPsw overexpressing cells. Thus, our *in vivo* and *in vitro* studies clearly show that high-dose zinc treatment enhances the amyloidogenic APP cleavage pathway and A $\beta$  secretion. Interestingly, a recent study involving APP/PS1 mice fed a zinc-deficient diet has shown that such a diet increases the plaque volume but does not alter the total plaque number in the brain [27]. Chronic high zinc- or copper-treated mice overexpress APP-C100, which contains A $\beta$  but not the N-terminal zinc and copper binding domain of APP, resulting in reduced soluble A $\beta$  levels but with no changes in the total A $\beta$  levels in the brain [54]. It has also been reported that exposure to copper and, presumably, a mixture of other metals in

drinking water results in enhanced A $\beta$  deposition in the brains of rabbits fed a high cholesterol diet [55]. Alain Boom and colleagues showed that 100  $\mu$ M zinc induced the appearance known to be associated with increased tau phosphorylation, suggesting that zinc plays a considerable role in the development of tau pathology associated to Alzheimer's disease [56]. On the other hand, some reports have shown the protective effects of low micromolar concentrations of zinc against A $\beta$  cytotoxicity [43,44,57]. So far, the role of zinc in AD remains debatable. Both high and low zinc could play a harmful role. Whether or not to supply zinc and what the suitable dose range should be are topics worthy of future research on AD. Taking these findings together with the present evidence that high-dose zinc treatment leads to enhanced amyloidogenic APP cleavage and A $\beta$  aggregation in the APP/PS1 mouse brain and APPsw overexpressing cells, it can be concluded that disturbed metal homeostasis is involved in multiple steps of APP processing and A $\beta$  deposition by a series of complicated mechanisms.

In summary, the present study provides evidence that chronic exposure to high zinc levels in drinking water leads to an increase in APP expression, amyloidogenic APP cleavage and A $\beta$  deposition in the APP/PS1 transgenic mouse brain. The present data, together with previous reports, suggest that excess zinc exposure could be a risk factor for AD pathological processes, and corrections of metal abnormalities in the brain are beneficial strategies for AD prevention and therapy.

## Materials and Methods

### Ethics statement

The experimental procedures were carried out in accordance with the regulations of the animal protection laws of China and approved by the animal ethics committee of China Medical University (JYT-20060948). All efforts were made to minimize animal suffering and the number of animals used.

### Animals and Treatments

Male APP/PS1 double transgenic mice (B6C3-Tg (APP<sup>sw</sup>, PSEN1<sup>dE9</sup>) 85Dbo/J mice) were used in the present study (breeding pairs were obtained from the Jackson Laboratory, West Grove, PA). They were kept in cages in a controlled environment (22–25°C, 50% humidity). Mice at the age of 3 months were randomly assigned to one of two groups (n = 12 in each group). (1) Control group: mice were given a standard diet (30 ppm zinc) and deionized water *ad libitum*. (2) Zinc group: mice were given a standard diet and deionized water containing ZnSO<sub>4</sub> (20 mg/ml). The doses of zinc chosen for this study were based on previous reports showing that it produced no serious toxicity in C57BL/6 mice after chronic treatment [33]. The potential toxicity of high-dose oral zinc on transgenic mice was evaluated by monitoring their general aspect and body weight. As reported previously [33,34], apart for a coat color change from black to bright brown on the back, and a decline in body weight starting from the 14th week after zinc treatment, no other overt signs of toxicity, such as general behavioral and neurological changes, were observed in mice on a high zinc diet during the entire observational period. At the age of 9 months, blood samples were drawn from the heart just prior to decapitation, and the levels of zinc in serum and brain were analyzed using a polarized Zeeman atomic absorption spectrophotometer (Hitachi 180-80, Japan).

### Morris Water Maze

Morris water maze tests were carried out as previously described with few modifications [58], using a circular tank, equipped with a

digital pick-up camera to monitor the animal behavior and a computer program for data analysis (ZH0065, Zhenghua Bio-equipments, China). Briefly, one week before reaching the age of 9 months, transgenic mice were trained for 2 days to remember the visible platform, which is placed in the center of the northwest quadrant in the tank with opaque water. From the 3rd to 7th day, the platform was placed just below the water surface (hidden platform) for the place navigation test, and each mouse was subjected to 3 trials per day with an inter-trial interval of 1 min. For each trial, the latency to escape to the hidden platform and the path length were recorded. At the 8th day, the platform was removed from the tank for the probe trial. The number of times the animal crossed the center of the northwest quadrant at an interval of 1 min was recorded. Finally, data for the escape latency, the path length and the number of passing times between groups were analyzed statistically.

### Tissue Preparation

The day after the Morris water maze tests, mice were anaesthetized with sodium pentobarbital (50 mg/kg, i.p.) and sacrificed by decapitation. The brains were removed immediately and split sagittally into halves. The left hemisphere was kept at  $-80^{\circ}\text{C}$  for Western blotting, RT-PCR or ELISA analyses. The right hemisphere was further cut into two slabs. One was immersed in 3% glutaraldehyde for zinc autometallographic analysis while the other was placed in 4% paraformaldehyde for immunohistochemical staining.

### Autometallography and Stereological Assessment

AMG was performed to analyze the distribution of zinc in the transgenic mouse brain according to our previous reports [20,59]. In brief, brain slices (2 mm) were cut with a vibratome and immersed in a mixture of 3% glutaraldehyde and 0.1% sodium sulfide at  $4^{\circ}\text{C}$  for 2 days. The slices were placed in 30% sucrose, frozen with liquid nitrogen and 30- $\mu\text{m}$  cryostat sections were prepared. Brain sections containing typical hippocampal structures from 2 groups were selected, placed in the same jar, and incubated in AMG developer at  $26^{\circ}\text{C}$  for 60 min. The AMG development was stopped by rinsing with 5% sodium thiosulfate for 10 min. After several washes with distilled water, the sections were dehydrated, covered with neutral balsam and examined with a light microscope equipped with a digital color camera. The sodium diethyldithiocarbamate trihydrate (DEDTC, Merck, 6689) control procedures were performed to ensure the specificity of the zinc ion staining [59].

The stereological assessment of zinc load in the AMG-stained brain sections was performed as reported previously [18], and this was carried out in matched brain areas from different groups. Briefly, a set of every 6th systematically sampled 30- $\mu\text{m}$ -thick AMG-stained sections of the transgenic mouse brain (yielding typically 5 sections/mouse) was selected. The total number of zinc-positive plaques was counted using the optical fractionator technique, while the area of zinc-positive plaques was analyzed in the same sections using the area fraction technique. The data were analyzed with Image-Pro Plus 6.0 software (Media Cybernetics, USA).

### Immunohistochemistry and A $\beta$ Load Measurements

Routine free floating ABC procedures were applied. Cryostat sections (30  $\mu\text{m}$ ) were treated with 3% hydrogen peroxide ( $\text{H}_2\text{O}_2$ ) in PB for 10 min to reduce endogenous peroxidase activity. After rinsing, the sections were treated with 5% bovine serum albumin and 3% goat serum in TBS for 1 h. They were then incubated with mouse anti-A $\beta$  (1:500, Sigma, A5213) overnight at  $4^{\circ}\text{C}$ . After

rinsing in TBS, the sections were incubated with 1:200 diluted biotinylated goat anti-mouse IgG for 1 h at room temperature (RT). The sections were then rinsed and treated with an ABC kit for 1 h at RT. The sections were rinsed in TBS and incubated with 0.025% 3, 3-diaminobenzidine (DAB) plus 0.0033%  $\text{H}_2\text{O}_2$  in TBS for 10 min. After rinsing, the sections were dehydrated, covered with neutral balsam, and examined with a light microscope. Control sections were incubated with normal serum instead of A $\beta$  antibody followed by all subsequent incubations as described above. The stereological assessment of A $\beta$  load in the A $\beta$ -immunostained brain sections was performed according to the above described procedure.

### Cell Culture and Drug Treatment

Human neuroblastoma SHSY-5Y cells stably transfected with human APP<sup>sw</sup> [28,29] were grown in DMEM supplemented with 10% heat-inactivated fetal calf serum, 100 U/ml penicillin, 100  $\mu\text{g}/\text{ml}$  streptomycin and 200  $\mu\text{g}/\text{ml}$  G418 at  $37^{\circ}\text{C}$  in humidified 5%  $\text{CO}_2$  air. Cells were incubated in serum-free medium for 2 h when they reached nearly 70% confluence. Then, cells were incubated with  $\text{ZnSO}_4$  (1  $\mu\text{M}$ , 70  $\mu\text{M}$ ), TPEN (1  $\mu\text{M}$ ) or  $\text{ZnSO}_4$  (70  $\mu\text{M}$ ) plus TPEN (1  $\mu\text{M}$ ) for 8 h. The concentrations of zinc and TPEN were selected based on routine MTT assay. To analyze the zinc entry into the cells, the staining with a zinc-specific fluorescent dye, Zinquin, was carried out by incubating the cells with 0.24  $\mu\text{M}$  Zinquin ethyl ester (Alexis, USA) for 30 min, and then examining them under a fluorescent microscope equipped with an image analysis system.

### Western Blotting

The preparation of lysates from the transgenic mouse brain samples and culture cells, and the Western blots were performed as described previously [19,21]. Briefly, samples were homogenized in an ice-cold lysis buffer. Each homogenate was centrifuged at 12,000 rpm for 30 min at  $4^{\circ}\text{C}$ , the supernatant was collected and the total protein levels were measured using a BCA protein assay kit. Proteins (50  $\mu\text{g}$ ) were separated on 8–15% SDS polyacrylamide gels according to the molecular weight of the detection proteins, and transferred onto PVDF membranes using an electron transfer device (45 V, overnight at  $4^{\circ}\text{C}$ ). The membranes were blocked with 5% non-fat milk in TBS containing 0.1% Tween-20 for 1 h and then incubated with a primary antibody for 2 h at room temperature. The primary antibodies used were: rabbit anti-ADAM10 (1:1000, Millipore, AB19026), rabbit anti-APP695 (1:4000, Chemicon, AB5352), rabbit anti-BACE1 (1:1000, Sigma, B0681); goat-anti-PS1 (1:1000, Millipore, MAB1563); mouse anti-sAPP $\alpha$  (1:500, IBM, 2B3, JP11088); mouse anti-sAPP $\beta$  (1:500, IBM, 6A1, JP10321); rabbit anti-APP-CTFs (1:4000, Sigma, A8717), and mouse anti-GAPDH (1:10000, KC-5G5, Kang Chen, 0811). Bound secondary antibodies were visualized using an enhanced chemiluminescence kit (Pierce, CA). Blots were repeated at least three times for every set of conditions. The band intensities were quantified using Image-pro Plus 6.0 analysis software.

### RT-PCR

Total RNA was isolated using Trizol reagent (Invitrogen) after homogenizing the brain tissue samples. The isolated RNA was examined by UV-spectroscopy at 260 nm. Total RNA (2  $\mu\text{g}$ ) of each sample was first transcribed to cDNA using a Reverse Transcription System kit (Promega, Madison, WI, USA). PCR amplification was performed with reagents from Promega. The cDNA solution was amplified with primers based on the human APP sequences. The primer sequences were: APP: 5'-GACT-

GACCACTCGACCAGGTTCTG-3' (upstream), 5'-CTTGAA-GTTGGATTCTCATACCG-3' (downstream); GAPDH: 5'-ACGGATTTGGTCGTATTGGG-3' (upstream), 5'-CGCTCCTGGAAGATGGTGAT-3' (downstream). Amplification was performed as follows: APP: 35 cycles of 95°C for 30 s, 62°C for 30 s and 72°C for 30 s; GAPDH: 30 cycles of 95°C for 45 s, 58°C for 45 s, and 72°C for 60 s. The PCR products were normalized in relation to standards of GAPDH mRNA. The results were determined and quantified with ChemDoc XRS Quantity One software.

## ELISA

A $\beta$  levels were determined using ELISA assay as described previously [21]. In brief, samples were placed in a 1:8 dilution of 5 M guanidine HCl/50 mM Tris HCl and thoroughly ground. The homogenate was diluted with dilution buffer containing an inhibitor protease complex and centrifuge at 12,000 rpm for 30 min at 4°C. The samples were then loaded on to 96-well plates and the level of A $\beta$  was determined using ELISA kits for A $\beta$ 1-40

## References

- Atwood CS, Huang X, Moir RD, Tanzi RE, Bush AI (1999) Role of free radicals and metal ions in the pathogenesis of Alzheimer's disease. *Met Ions Biol Syst* 36: 309–364.
- Bush AI (2000) Metals and neuroscience. *Curr Opin Chem Biol* 4: 184–191.
- Maynard CJ, Bush AI, Masters CL, Cappai R, Li QX (2005) Metals and amyloid-beta in Alzheimer's disease. *Int J Exp Pathol* 86: 147–159.
- Barnham KJ, Bush AI (2008) Metals in Alzheimer's and Parkinson's diseases. *Curr Opin Chem Biol* 12: 222–228.
- Lovell MA, Robertson JD, Teesdale WJ, Campbell JL, Markesbery WR (1998) Copper, iron and zinc in Alzheimer's disease senile plaques. *J Neurol Sci* 158: 47–52.
- Cherny RA, Legg JT, McLean CA, Fairlie DP, Huang X, et al. (1999) Aqueous dissolution of Alzheimer's disease Abeta amyloid deposits by biometal depletion. *J Biol Chem* 274: 23223–23228.
- Suh SW, Jensen KB, Jensen MS, Silva DS, Kesslak PJ, et al. (2000) Histochemically-reactive zinc in amyloid plaques, angiopathy, and degenerating neurons of Alzheimer's diseased brains. *Brain Res* 852: 274–278.
- Dong J, Atwood CS, Anderson VE, Siedlak SL, Smith MA, et al. (2003) Metal binding and oxidation of amyloid-beta within isolated senile plaque cores: Raman microscopic evidence. *Biochemistry* 42: 2768–2773.
- Friedlich AL, Lee JY, van Groen T, Cherny RA, Volitakis I, et al. (2004) Neuronal zinc exchange with the blood vessel wall promotes cerebral amyloid angiopathy in an animal model of Alzheimer's disease. *J Neurosci* 24: 3453–3459.
- Stoltenberg M, Bruhn M, Sondergaard C, Doering P, West MJ, et al. (2005) Immersion autometallographic tracing of zinc ions in Alzheimer beta-amyloid plaques. *Histochem Cell Biol* 123: 605–611.
- Bush AI, Pettingell WH, Multhaup G, d Paradis M, Vonsattel JP, et al. (1994) Rapid induction of Alzheimer A beta amyloid formation by zinc. *Science* 265: 1464–1467.
- Cherny RA, Atwood CS, Xilinas ME, Gray DN, Jones WD, et al. (2001) Treatment with a copper-zinc chelator markedly and rapidly inhibits beta-amyloid accumulation in Alzheimer's disease transgenic mice. *Neuron* 30: 665–676.
- Bush AI (2002) Metal complexing agents as therapies for Alzheimer's disease. *Neurobiol Aging* 23: 1031–1038.
- Lee JY, Friedman JE, Angel I, Kozak A, Koh JY (2004) The lipophilic metal chelator DP-109 reduces amyloid pathology in brains of human beta-amyloid precursor protein transgenic mice. *Neurobiol Aging* 25: 1315–1321.
- Ritchie CW, Bush AI, MacKinnon A, Macfarlane S, Mastwyk M, et al. (2003) Metal-protein attenuation with iodochlorhydroxyquin (clioquinol) targeting Abeta amyloid deposition and toxicity in Alzheimer disease: a pilot phase 2 clinical trial. *Arch Neurol* 60: 1685–1691.
- Jenagaratnam L, McShane R (2006) Clioquinol for the treatment of Alzheimer's Disease. *Cochrane Database Syst Rev*: CD005380.
- Price KA, Crouch PJ, White AR (2007) Therapeutic treatment of Alzheimer's disease using metal complexing agents. *Recent Pat CNS Drug Discov* 2: 180–187.
- Zhang LH, Wang X, Stoltenberg M, Danscher G, Huang L, et al. (2008) Abundant expression of zinc transporters in the amyloid plaques of Alzheimer's disease brain. *Brain Res Bull* 77: 55–60.
- Zhang LH, Wang X, Zheng ZH, Ren H, Stoltenberg M, et al. (2010) Altered expression and distribution of zinc transporters in APP/PS1 transgenic mouse brain. *Neurobiol Aging* 31: 74–87.
- Zheng W, Wang T, Yu D, Feng WY, Nie YX, et al. (2010) Elevation of zinc transporter ZnT3 protein in the cerebellar cortex of the AbetaPP/PS1 transgenic mouse. *J Alzheimers Dis* 20: 323–331.
- Zheng W, Xin N, Chi ZH, Zhao BL, Zhang J, et al. (2009) Divalent metal transporter 1 is involved in amyloid precursor protein processing and Abeta generation. *FASEB J* 23: 4207–4217.
- Lovell MA, Smith JL, Xiong S, Markesbery WR (2005) Alterations in zinc transporter protein-1 (ZnT-1) in the brain of subjects with mild cognitive impairment, early, and late-stage Alzheimer's disease. *Neurotox Res* 7: 265–271.
- Lovell MA, Smith JL, Markesbery WR (2006) Elevated zinc transporter-6 in mild cognitive impairment, Alzheimer disease, and pick disease. *J Neuropathol Exp Neurol* 65: 489–498.
- Cole TB, Wenzel HJ, Kafer KE, Schwartzkroin PA, Palmiter RD (1999) Elimination of zinc from synaptic vesicles in the intact mouse brain by disruption of the ZnT3 gene. *Proc Natl Acad Sci U S A* 96: 1716–1721.
- Adlard PA, Parncutt JM, Finkelstein DI, Bush AI (2010) Cognitive loss in zinc transporter-3 knock-out mice: a phenocopy for the synaptic and memory deficits of Alzheimer's disease? *J Neurosci* 30: 1631–1636.
- Lee JY, Cole TB, Palmiter RD, Suh SW, Koh JY (2002) Contribution by synaptic zinc to the gender-disparate plaque formation in human Swedish mutant APP transgenic mice. *Proc Natl Acad Sci U S A* 99: 7705–7710.
- Stoltenberg M, Bush AI, Bach G, Smidt K, Larsen A, et al. (2007) Amyloid plaques arise from zinc-enriched cortical layers in APP/PS1 transgenic mice and are paradoxically enlarged with dietary zinc deficiency. *Neuroscience* 150: 357–369.
- Zhang J, Liu Q, Chen Q, Liu NQ, Li FL, et al. (2006) Nicotine attenuates beta-amyloid-induced neurotoxicity by regulating metal homeostasis. *FASEB J* 20: 1212–1214.
- Zhang J, Mori A, Chen Q, Zhao B (2006) Fermented papaya preparation attenuates beta-amyloid precursor protein: beta-amyloid-mediated copper neurotoxicity in beta-amyloid precursor protein and beta-amyloid precursor protein Swedish mutation overexpressing SH-SY5Y cells. *Neuroscience* 143: 63–72.
- Borchardt T, Schmidt C, Camarkis J, Cappai R, Masters CL, et al. (2000) Differential effects of zinc on amyloid precursor protein (APP) processing in copper-resistant variants of cultured Chinese hamster ovary cells. *Cell Mol Biol (Noisy-le-grand)* 46: 785–795.
- Cuajungco MP, Faget KY (2003) Zinc takes the center stage: its paradoxical role in Alzheimer's disease. *Brain Res Brain Res Rev* 41: 44–56.
- Bush AI, Multhaup G, Moir RD, Williamson TG, Small DH, et al. (1993) A novel zinc(II) binding site modulates the function of the beta A4 amyloid protein precursor of Alzheimer's disease. *J Biol Chem* 268: 16109–16112.
- Plonka PM, Handjiski B, Popik M, Michalczyk D, Paus R (2005) Zinc as an ambivalent but potent modulator of murine hair growth in vivo—preliminary observations. *Exp Dermatol* 14: 844–853.
- Plonka PM, Handjiski B, Michalczyk D, Popik M, Paus R (2006) Oral zinc sulphate causes murine hair hypopigmentation and is a potent inhibitor of eumelanogenesis in vivo. *Br J Dermatol* 155: 39–49.
- Miller LM, Wang Q, Telivala TP, Smith RJ, Lanzirotti A, et al. (2006) Synchrotron-based infrared and X-ray imaging shows focalized accumulation of Cu and Zn co-localized with beta-amyloid deposits in Alzheimer's disease. *J Struct Biol* 155: 30–37.
- Lee JY, Mook-Jung I, Koh JY (1999) Histochemically reactive zinc in plaques of the Swedish mutant beta-amyloid precursor protein transgenic mice. *J Neurosci* 19: RC10.

37. Bush AI, Pettingell WH, Jr., Paradis MD, Tanzi RE (1994) Modulation of A beta adhesiveness and secretase site cleavage by zinc. *J Biol Chem* 269: 12152–12158.
38. Dineley KE, Votyakova TV, Reynolds IJ (2003) Zinc inhibition of cellular energy production: implications for mitochondria and neurodegeneration. *J Neurochem* 85: 563–570.
39. Dineley KE, Richards LL, Votyakova TV, Reynolds IJ (2005) Zinc causes loss of membrane potential and elevates reactive oxygen species in rat brain mitochondria. *Mitochondrion* 5: 55–65.
40. Sensi SL, Ton-That D, Sullivan PG, Jonas EA, Gee KR, et al. (2003) Modulation of mitochondrial function by endogenous Zn<sup>2+</sup> pools. *Proc Natl Acad Sci U S A* 100: 6157–6162.
41. Sensi SL, Paoletti P, Bush AI, Sekler I (2009) Zinc in the physiology and pathology of the CNS. *Nat Rev Neurosci* 10: 780–791.
42. Lovell MA, Xie C, Markesbery WR (1999) Protection against amyloid beta peptide toxicity by zinc. *Brain Res* 823: 88–95.
43. Cuajungco MP, Goldstein LE, Nunomura A, Smith MA, Lim JT, et al. (2000) Evidence that the beta-amyloid plaques of Alzheimer's disease represent the redox-silencing and entombment of abeta by zinc. *J Biol Chem* 275: 19439–19442.
44. Yoshiike Y, Tanemura K, Murayama O, Akagi T, Murayama M, et al. (2001) New insights on how metals disrupt amyloid beta-aggregation and their effects on amyloid-beta cytotoxicity. *J Biol Chem* 276: 32293–32299.
45. Lue LF, Kuo YM, Roher AE, Brachova L, Shen Y, et al. (1999) Soluble amyloid beta peptide concentration as a predictor of synaptic change in Alzheimer's disease. *Am J Pathol* 155: 853–862.
46. McLean CA, Cherny RA, Fraser FW, Fuller SJ, Smith MJ, et al. (1999) Soluble pool of Abeta amyloid as a determinant of severity of neurodegeneration in Alzheimer's disease. *Ann Neurol* 46: 860–866.
47. Wang J, Dickson DW, Trojanowski JQ, Lee VM (1999) The levels of soluble versus insoluble brain Abeta distinguish Alzheimer's disease from normal and pathologic aging. *Exp Neurol* 158: 328–337.
48. Kozin SA, Zirah S, Rebuffat S, Hoa GH, Debey P (2001) Zinc binding to Alzheimer's Abeta(1-16) peptide results in stable soluble complex. *Biochem Biophys Res Commun* 285: 959–964.
49. Tougu V, Karafin A, Palumaa P (2008) Binding of zinc(II) and copper(II) to the full-length Alzheimer's amyloid-beta peptide. *J Neurochem* 104: 1249–1259.
50. Cuajungco MP, Lees GJ (1996) Prevention of zinc neurotoxicity in vivo by N,N,N',N'-tetrakis (2-pyridylmethyl) ethylene-diamine (TPEN). *Neuroreport* 7: 1301–1304.
51. Cuajungco MP, Lees GJ (1998) Diverse effects of metal chelating agents on the neuronal cytotoxicity of zinc in the hippocampus. *Brain Res* 799: 97–107.
52. Garai K, Sahoo B, Kaushalya SK, Desai R, Maiti S (2007) Zinc lowers amyloid-beta toxicity by selectively precipitating aggregation intermediates. *Biochemistry* 46: 10655–10663.
53. Smedman M, Potempska A, Rubenstein R, Ju W, Ramakrishna N, et al. (1997) Effects of cadmium, copper, and zinc and beta APP processing and turnover in COS-7 and PC12 cells. Relationship to Alzheimer disease pathology. *Mol Chem Neuropathol* 31: 13–28.
54. Maynard CJ, Cappai R, Volitakis I, Loughton KM, Masters CL, et al. (2009) Chronic exposure to high levels of zinc or copper has little effect on brain metal homeostasis or Abeta accumulation in transgenic APP-C100 mice. *Cell Mol Neurobiol* 29: 757–767.
55. Sparks DL, Schreurs BG (2003) Trace amounts of copper in water induce beta-amyloid plaques and learning deficits in a rabbit model of Alzheimer's disease. *Proc Natl Acad Sci U S A* 100: 11065–11069.
56. Boom A, Authelat M, Dedecker R, Frederick C, Van Heurck R, et al. (2009) Bimodal modulation of tau protein phosphorylation and conformation by extracellular Zn<sup>2+</sup> in human-tau transfected cells. *Biochim Biophys Acta* 1793: 1058–1067.
57. Cardoso SM, Rego AC, Pereira C, Oliveira CR (2005) Protective effect of zinc on amyloid-beta 25-35 and 1-40 mediated toxicity. *Neurotox Res* 7: 273–281.
58. Qing H, He G, Ly PT, Fox CJ, Staufenbiel M, et al. (2008) Valproic acid inhibits Abeta production, neuritic plaque formation, and behavioral deficits in Alzheimer's disease mouse models. *J Exp Med* 205: 2781–2789.
59. Danscher G, Stoltenberg M (2006) Silver enhancement of quantum dots resulting from (1) metabolism of toxic metals in animals and humans, (2) in vivo, in vitro and immersion created zinc-sulphur/zinc-selenium nanocrystals, (3) metal ions liberated from metal implants and particles. *Prog Histochem Cytochem* 41: 57–139.